

Realistic simulation of breast mass appearance using random walk

Alaleh Rashidnasab^{*a}, Premkumar Elangovan^a, David R Dance^{b,c}, Kenneth C Young^{b,c}, Mary Yip^c, Oliver Diaz^a, Kevin Wells^a

^a Centre for Vision, Speech and Signal Processing, University of Surrey,
Guildford, GU2 7XH, UK

^b Department of Physics, , University of Surrey, Guildford, GU2 7XH, UK

^c National Coordinating Centre for the Physics of Mammography, Royal Surrey County
Hospital, Guildford, GU2 7XX, UK

ABSTRACT

The aim of the present work was to develop a method for simulating breast lesions in digital mammographic images. Based on the visual appearance of real masses, three dimensional masses were created using a 3D random walk method where the choice of parameters (number of walks and number of steps) enables one to control the appearance of the simulated structure. This work is the first occasion that the random walk results have been combined with a model of digital mammographic imaging systems. This model takes into account appropriate physical image acquisition processes representing a particular digital X-ray mammography system. The X-ray spectrum, local glandularity above the insertion site and scatter were all taken account during the insertion procedure. A preliminary observer study was used to validate the realism of the masses. Seven expert readers each viewed 60 full field mammograms and rated the realism of the masses they contained. Half of the images contained real, histologically-confirmed masses, and half contained simulated lesions. The ROC analysis of the study (average *AUC* of 0.58±0.06) suggests that, on the average, there is evidence that the radiologists could distinguish, somewhat, between real and simulated masses.

Keywords: simulation, mammography, lesion modelling

1. INTRODUCTION

X-ray mammography is currently the imaging modality of choice in screening to detect breast cancer in the early stages [1]. However, the effectiveness of the detection task depends critically on the quality of the mammographic image and the radiologist's level of experience and skill. In recent years, film-screen systems have been replaced by various digital mammography technologies as these can deliver better performance than conventional film-screen technology [2]. However it remains unclear how the physical performance of such systems and the choice of their operating parameters is correlated with ability to detect early breast cancer. Clinical trials are an obvious response to this issue, but these are costly and take many years to conclude. They also rely on the availability of a large number of images with pathologically-proven lesions. Alternatively, a simulation framework whereby suitably-realistic synthetic breast cancer pathology is inserted into normal clinical mammograms to form a large database can enable a more efficient comparison of multiple systems and study of technical parameters which influence the detection task.

This paper describes the use of random walks to simulate the radiographic appearance of masses in digital mammography. In distinction to previous work in this area [4,5], there is no *ad-hoc* morphological processing of the simulated masses. Instead, the random walks are undertaken at a pseudo-mesoscopic scale, and then processed taking account of beam-dependent attenuation factors, the image receptor modulation transfer function (MTF), pixel sampling and scatter. Account is also taken of the local breast glandularity to ensure that the contrast of the simulated mass is realistic when inserted into a mammogram.

*Further author information: (Send correspondence to Alaleh Rashidnasab)

Email: a.rashidnasab@surrey.ac.uk

2. METHODOLOGY

The simulation framework as shown in Figure 1 is divided into several steps: (1) simulation of a 3D mass based on nearest-neighbor random walk, (2) calculation of the primary transmission through the breast before and after mass insertion using local glandularity information [8], (3) degradation of the projected mass with the appropriate MTF and resampling to the pixel size of the particular digital mammography image acquisition system, (4) insertion of the mass into the raw clinical mammogram also considering scatter, and finally processing the image with manufacturer-specific image processing package. The following subsections describe these steps in more detail.

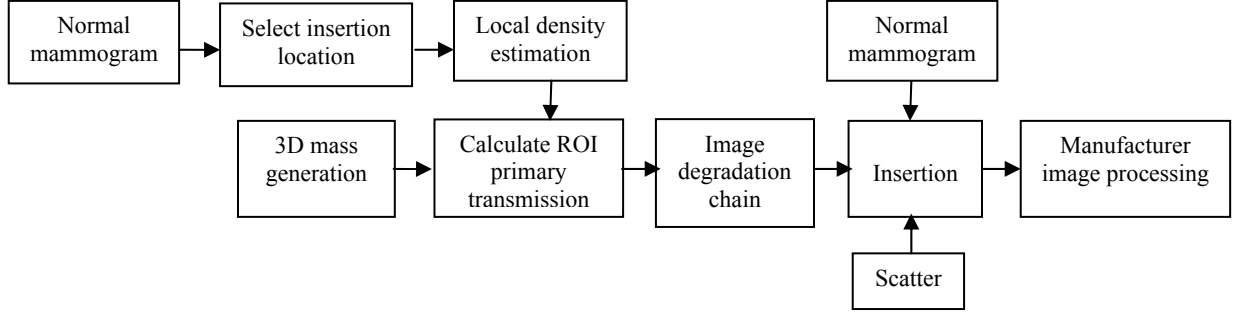


Figure 1. Overall image simulation framework of simulation disease in digital mammograms

2.1 Mass simulation

To generate a malignant mass, a nearest neighbour random walk algorithm for simulating 3D masses was developed based on the work by Ruschin et al [4] and Histsala et al[5]. Initially the random walk starts by incrementing the value of the centre voxel of a binary 3D array indicating the mass centre. In each iteration, one of the connected voxels in the 26 way local neighbourhood is chosen randomly from a uniform distribution and incremented by assigning unit value. If a voxel was revisited more than once during the walk the unit value is not incremented. The walk proceeds in a random direction until it reaches a preset number of steps (n) or it intersects a bounding box boundary defined by the user. The procedure then repeats from the same starting point for a given number of recursions (R). The R and n parameters enable the user to control the size and relative density or “texture” of the generated mass. The bounding box limits the random walk to a user-defined shape. The voxel size was $17.5\mu\text{m}$ and a range of 5 to 15 mm masses were simulated.

2.2 Calculation of primary transmission

The process used for insertion of a mass into a mammogram requires knowledge of the relative signals from primary photons in the region of interest (ROI) where the mass is to be inserted. The ROI on the normal mammogram was selected manually based on local morphology and visual appearance. Both Primary photons before (p_1) and after (p_2) insertion of the mass were calculated for a parallel beam geometry and X-ray spectrum $N(E)$ using:

$$p_1 = \sum_E E \epsilon(E) N(E) e^{-\sum_i \mu_i(E) t_i - \mu_{br}(E) t_{br}} \Delta E \quad (1)$$

$$p_2 = \sum_E E \epsilon(E) N(E) e^{-\sum_i \mu_i(E) t_i - \mu_{br}(E) t_{br} - \mu_{mass}(E) t_{mass} + \mu_{br}(E) t_{mass}} \Delta E \quad (2)$$

In these equations, $\epsilon(E)$ is the detector energy absorption efficiency as a function of photon energy (E), the X-ray number spectra $N(E)$ were calculated from the spectral model of Boone et al. [10], and corresponded to the specific target/filter combination, tube voltage, filter thickness used during image acquisition of the associated mammogram. ΔE is the bin size of the X-ray spectrum and the summation within each exponential term is over the different materials of attenuation coefficient μ_i and thickness t_i traversed by the beam along its trajectory including compression paddle. μ_{br} is the breast tissue attenuation coefficient and t_{br} is the thickness of breast along the beam. The linear attenuation coefficients were calculated using data from NIST [11]. The breast tissue along the path of each primary photon was assumed to comprise a mixture of adipose and glandular tissues, and the composition of these tissues was taken from the work of Hammerstein et al [14]. The linear attenuation coefficient of glandular tissue was also used for the 3D simulated mass, which was assumed to be homogeneous. In order to estimate the

glandularity of the breast region above each image pixel for calculation of μ_{br} , Volpara was employed [8,9]. Volpara is a breast composition measurement tool which uses relative physics modelling by finding an area of the breast that corresponds to entirely fatty tissue as a reference level to find the thickness of dense tissue at each pixel of the mammogram. The use of Volpara facilitated more accurate tissue replacement when inserting a mass compared to global or other approximations of glandularity which would otherwise be required. The third term in Eq.3 accounts for the mass inserted and the last term accounts for the replaced tissue. It is assumed that the mass voxels within the 3D array are enclosed in a breast tissue with same attenuation coefficient as μ_{br} .

2.3 Image degradation chain

Prior work on mass simulation using random walk methods [4,5] has empirically used morphological image processing to achieve a visually satisfactory appearance when inserting the simulated masses into digitized film-screen masses [4] or a simulated breast model [5]. However in the present work, the resulting 2D arrays calculated above (p_1 and p_2) were blurred and sampled using the approach of Yip et al [3] representing the image degradation process associated with commercially available digital mammography systems. Thus the primary projections were blurred according to the particular system MTF and the resultant image resampled at the system's detector pixel size to produce the arrays $p_{1modified}$ and $p_{2modified}$. The ratio of these two quantities, which we call the relative transmission factor, was also calculated.

2.4 Mass insertion, Scatter and Processing

The scatter to primary ratio (SPR) was estimated and used in the insertion model with the following steps: remove the scatter, adjust the primary transmission due to insertion of a mass, and then re-instate the scatter, assuming the effect of mass insertion has negligible effect on the slowly varying scatter field. The mass insertion can now be performed by calculating the value of each pixel in the ROI using Eq.3:

$$I_2 = \frac{I_1}{(1+SPR)} \times \frac{p_{2modified}}{p_{1modified}} \left(1 + SPR \times \frac{p_{1modified}}{p_{2modified}} \right) \quad (3)$$

where I_1 is the raw input image in the ROI before insertion, and I_2 is the output image after insertion of the simulated mass. The SPR is a single value estimated for the whole mammogram for the specific breast thickness and glandularity of the associated mammogram prior to mass insertion.

In order to calculate the SPR for equation (3), Monte Carlo simulation was used for a range of breast thicknesses and glandularities, and then these data were interpolated to estimate SPR values for any image used in the study. As all the images in this study were acquired by Hologic Selenia systems, accordingly this system geometry was used during the simulation, including compression paddle, breast support and anti-scatter grid. Breast phantoms have been modelled as uniform semicircles of different heights and diameters. 10^9 photons emerging from a point source at 66cm from the detector have been used for each simulation, irradiating the entire receptor's dimension. Primary and scattered photons were recorded in a region of interest of area 1cm^2 at 6cm from the chest wall and SPR calculated specifically for this study using the methodology described in [12].

The resultant image was then processed by the relevant manufacturer's post acquisition image processing package routinely used for image enhancement.

2.5 Validation of the simulation

2.5.1 Subjective pilot study

A pilot study was used to improve the simulation model and to guide realistic parameter selection for the more detailed ROC validation study. Sixteen normal mammograms each containing a simulated mass were reviewed by three expert radiologists who were asked to evaluate the realism of the simulated masses in terms of their shape, margin, density and type of malignancy. The pilot study results suggested that random walk masses for a given range of parameters are capable of producing realistic results.

2.5.2 Preliminary Observer Study

An observer study was performed to evaluate whether radiologists could distinguish real masses from inserted simulated masses. Sixty single view full-field images were used in the study (MLO or CC views). Half contained real pathology-proven masses and half were normal mammograms into which a simulated mass had been inserted. All the images used in the study were routine breast screening images acquired on Hologic Selenia systems at the

Jarvis Breast Screening Centre, Guildford and St. Georges Hospital, London. Seven radiologists with an average of six years experience in breast screening, acted as readers.

The images were shown in a random order to each radiologist. No information was provided about the number of masses in each category, but the approximate location of the mass within the image was indicated. Radiologists were asked to rank the realism of the mass on a 5-point scale such that 1: definitely simulated, 2: probably simulated, 3: indeterminate, 4: probably real and 5: definitely real. They were also asked to rank the level of suspicion of the mass on a 5-point scale used in clinical assessments, i.e. 1: normal, 2: benign, 3: indeterminate, 4: suspicious and 5: malignant. Receiver operating characteristic (ROC) analysis [6] was performed in order to assess the readers' ability to distinguish between simulated and real masses.

A teaching dataset was used in the beginning of each study to familiarise the observers with the in-house software specifically designed for the validation study using a Java-based Plug-In for ImageJ [15]. This software provided move, zoom, and hide/show location of the mass options. All the studies were performed on a high resolution 5 megapixel monitor specific for mammography under the same lighting conditions as used in routine screening sessions. There was no time constraint placed on the image assessment.

3. RESULTS AND DISCUSSION

Figure 2 shows three examples of simulated masses and the normal mammogram before and after insertion. Breast tissue is partially visible through the simulated masses as the masses blend well with the corresponding original mammographic architecture (Fig 3 (g-i) magnified views).

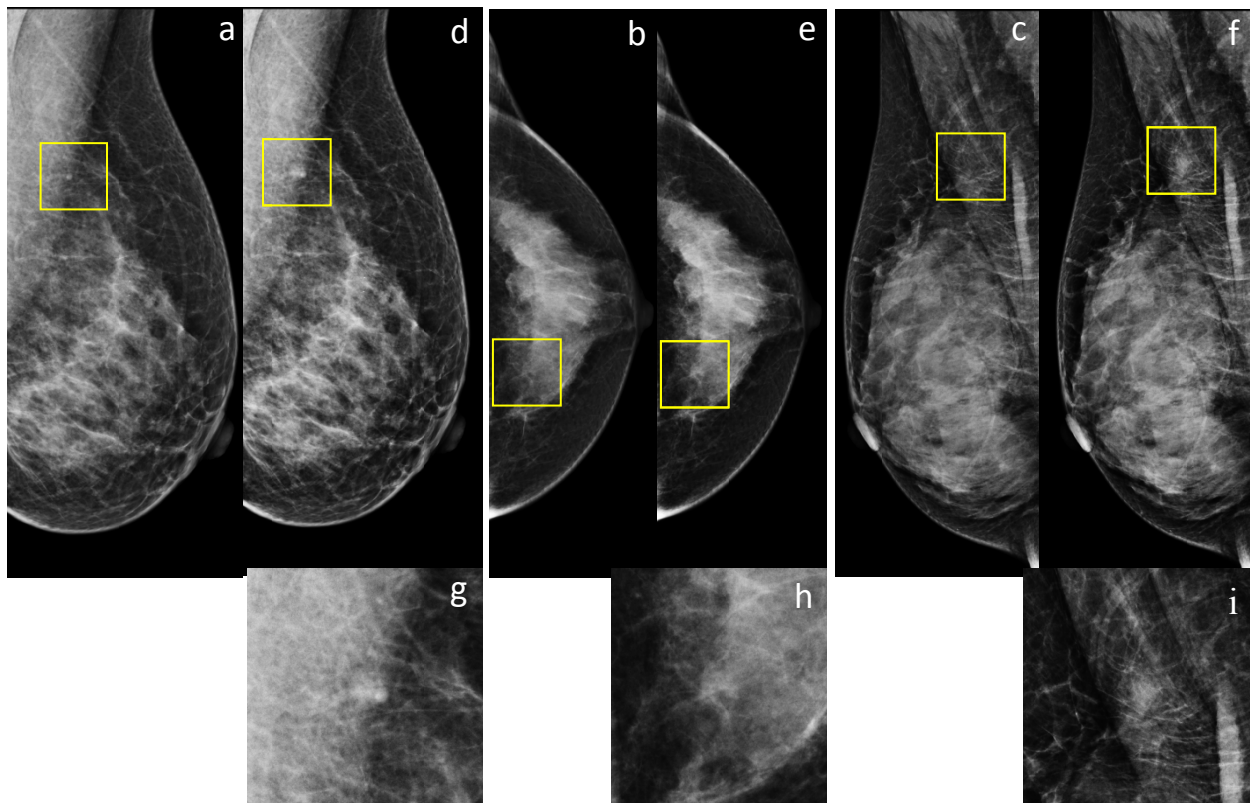


Figure 2. Examples of simulated masses. Images acquired using an Hologic Selenia mammography system and processed with Hologic image processing package (LORAD FFDM Selenia v 5.0). (a-c) shows normal digital mammograms before inserting masses. The yellow boxes indicate the selected ROIs for mass insertion, (d-f) mammograms from (a-c) after mass insertion. The mass is located at the centre of yellow box. (g-i) magnified version of insertion ROIs.

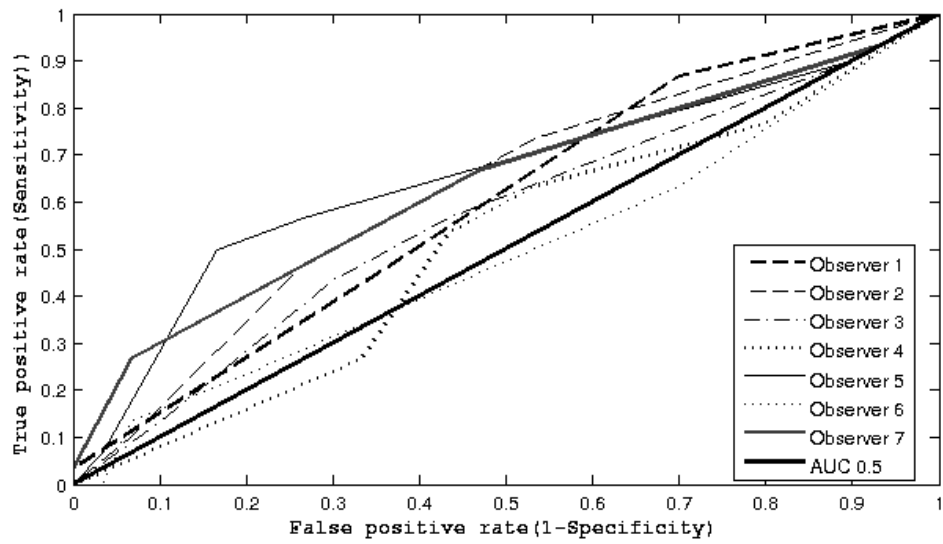


Figure 3. ROC curves of the simulated masses study per observer

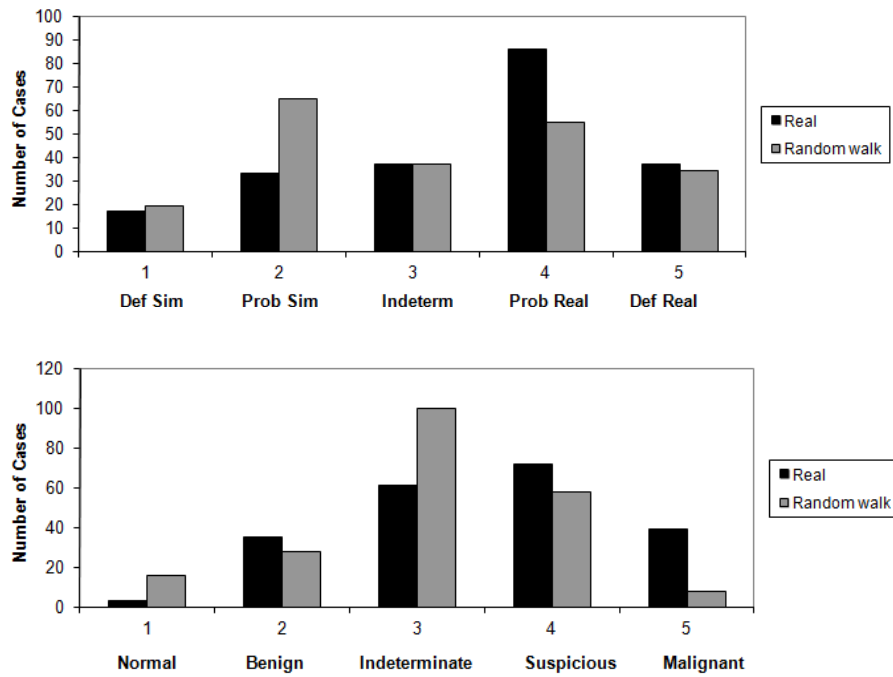


Figure 4. Global histogram of all the observers for the real and the simulated masses ranking (top). Global histogram of level of suspicion scores for all the observers (bottom).

Table1. Area under the ROC curve (AUC) and associated 95% CI per observer; the last row gives the average AUC over all readers and corresponding 95% CI.

<i>Observer</i>	<i>Area Under Curve</i>	<i>95% CI</i>
Observer1	0.59	(0.45 , 0.74)
Observer2	0.62	(0.48 , 0.77)
Observer3	0.57	(0.42 , 0.71)
Observer4	0.51	(0.36 , 0.65)
Observer5	0.65	(0.51 , 0.79)
Observer6	0.49	(0.34 , 0.63)
Observer7	0.63	(0.49 , 0.77)
Average	0.58	(0.52, 0.64)

Figure 3 presents the ROC curves from the observer study for each radiologist. The 50-50 chance line is shown in black. Table 1 gives the areas under the ROC Curves (AUCs) computed using the trapezoidal rule along with the 95% confidence interval (CI) for each reader [13]. The average AUC over all readers and corresponding 95% CIs are also shown. The results from table 1 demonstrate that except for one reader all the CIs include the value 0.5, and thus the remaining radiologists could not tell the difference between real and simulated masses. The CI for the average AUC, calculated using standard error for seven AUCs, resulted in (0.52, 0.64). As the overall CI does not include the value 0.5, this suggests that, on the average, there is evidence that the radiologists could distinguish, somewhat, between real and simulated masses. However the low number of samples within this study affects the CI results, requiring larger statistics to determine the validity of this conclusion.

Figure 4(top) shows that despite the results from AUC and CI, the random walk method is capable of producing realistic results in some cases. Figure 4(bottom) shows the overall histogram of all observers for the level of suspicion ranking. In the UK, clinical assessment of screening images requires a recall if the level of suspicion of the detected mass is rated as 3 or more. Comparing the results on the global histogram, the number of recalls (summation of last 3 bars) for real cases is 172(82% of all the real masses) and 166 for simulated cases (79% of all the simulated masses) which are comparable. This result shows that for the limitations imposed by the limited statistics of this study, the simulation method was successful in creating masses with a realistic malignant appearance.

4. CONCLUSION

A method has been described using random walks to simulate the appearance of lesions in digital X-ray mammography images. In contrast to prior work, no *ad-hoc* morphological processing is needed, as this is replaced with a physics-based image simulation chain to degrade the pseudo-mesoscopic random walk with the appropriate major physical sources of image degradation during image acquisition. We have presented a preliminary assessment of the appearance of these masses; ROC analysis was performed on 30 real cancer images and 30 images with simulated cancers. The result from the observer study shows that the average AUC did not included 0.5 and thus, this limited study suggests that observers could distinguish between real and simulated images in a number of cases. However half of the simulated masses were rated as real by the radiologist suggesting that it may be possible to create realistic lesions using this approach with further development and validation.

ACKNOWLEDGMENTS

This work is part of the OPTIMAM project and is supported by the CR-UK & EPSRC Cancer Imaging Programme in Surrey, in association with the MRC and Department of Health (England).

The authors thanks Ralph Highnam for granting access to the Volpara breast volume measurement tool and providing technical assistance. The authors would also like to thank colleagues at NCCPM, the clinical observers at Jarvis Breast Screening Centre, Guildford, St. Georges Hospital, London and Addenbrookes Hospital, Cambridge and especially Dr. Julie Cooke for their invaluable assistant.

REFERENCES

- [1] Heywang-Kobrunner, S., Dershaw, D. D. and Schreer, I., [Diagnostic breast imaging], 2nd ed., Thieme publications, (2001).
- [2] Young, K. and Dance, D., [Contemporary issues in cancer imaging: Breast cancer- Chapter4: Advances in X-ray mammography], Cambridge Uni. press, (2010).
- [3] Yip, M., Mackenzie, A., Lewis, E., Dance, D. R., Young, K. C., Christmas, W. and Wells, K., "Image resampling effects in mammographic image simulation," *Physics in Medicine and Biology* 56(22), 275-286 (2011).
- [4] Ruschin, M., Tingberg, A., Bth, M., Grahn, A., Hkansson, M., Hemdal, B. and Andersson, I., "Using simple mathematical functions to simulate pathological structures- input for digital mammography clinical trial," *Radiation Protection Dosimetry* 114(1-3):424-431(2005).
- [5] Hintsala, H., Bliznakova, K., Pallikarakis, N. and Jämsä, T., "Modelling of irregular breast lesions," *Proc IFMBE*, 2024-2027 (2009).
- [6] Barrett, H. H. and Myers, K. J., [Foundation of image science], John Wiley & Sons publications, (2004).
- [7] Saunders, R., Samei, E., Baker, J. and Delong, D., "Simulation of mammographic lesions," *Academic Radiology* 13(7), 860-870 (2006).
- [8] Highnam, R., Brady, M., Yaffe, M. J., Karssemeijer, N. and Harvey, J., "Robust breast composition measurements – Volpara," *Proc. International Workshop on Digital Mammography*, 342-349 (2010).
- [9] Highnam, R., Pan, X., Warren, R., Je Reys, M., Smith, G. and Brady, M., "Breast composition measurements using retrospective standard mammogram form (smf)," *Physics in Medicine and Biology* 51, 2695–2713 (2006).
- [10] Boone, J. M., Fewell, T. R. and Jennings, R. J., "Molybdenum, rhodium, and tungsten anode spectral models using interpolating polynomials with application to mammography," *Medical Physics* 24(12), 1863-1874 (1997).
- [11] NIST XCOM, <http://physics.nist.gov/PhysRefData/Xcom/html/xcom1.html>
- [12] Diaz, O., Yip, M., Cabello, J., Dance, D. R., Young, K. C. and Wells, K., "Monte Carlo simulation of scatter field for calculation of contrast of discs in synthetic CDMAM images", *Proc. International Workshop on Digital Mammography*, 628-635 (2010).
- [13] Hanley, J. A. and McNeil, B. J., "The meaning and use of the area under a receiver operating characteristic (roc) curve", *Radiology* 143(1), 29-36 (1982).
- [14] Hammerstein, G. R., Miller, D. W., White, D. R., Masterson, M. E., Woodard, H. Q. and Laughlin, J. S., "Absorbed radiation dose in mammography," *Radiology* 130, 485-489 (1979).
- [15] Abramoff, M. D., Magelhaes, P. J. and Ram, S. J., "Image processing with ImageJ," *Biophotonics International* 11(7), 36-42 (2004).